Environmental Science & Technology

pubs.acs.org/est

Article

Protein-Affinity-Guided Identification of Bioaccumulative Silanol Quaternary Ammonium Compounds in Indoor Environments and Human Serum

Yao Cheng,[†] Zhong Lv,[†] Haoran Xia, Xiaoyuan Guo, Xiaozhen Zhang, Baoqin Huang, Bixuan Wang, Zhaomin Dong, Da Chen,* and Guomao Zheng*

Cite This: https://doi.org/10.1021/acs.est.5c13764

Read Online

ACCESS | Metrics & More | Article Recommendations | Supporting Information

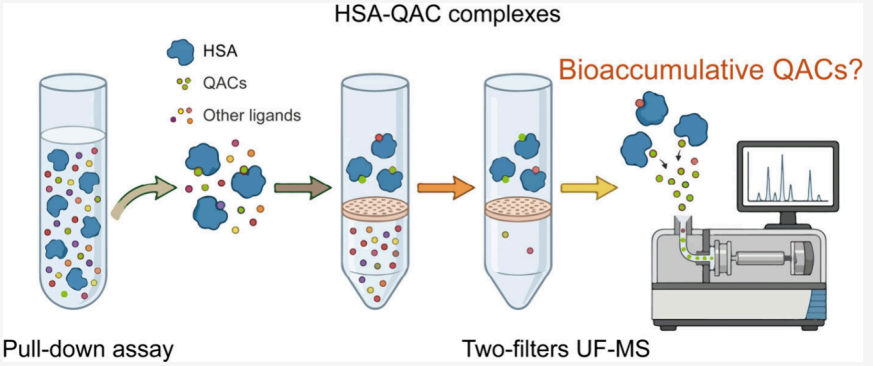

ABSTRACT: Quaternary ammonium compounds (QACs) have raised concerns due to their widespread use in disinfectants and unknown bioaccumulation behavior. However, conventional bioaccumulation assessments are costly, time-consuming, and low-throughput, limiting their utility for screening the growing array of emerging QACs. In this study, we developed a protein affinity ultrafiltration mass spectrometry (PA-UF-MS) strategy using human serum albumin (HSA) as a molecular bait to selectively isolate bioaccumulative QACs from disinfectants. We identified 12 traditional and emerging QACs, including several silanol alkyltrimethylammonium compounds (silanol-ATMACs), with strong HSA binding affinities [fold changes (FCs): 10.1−60.0]. Five silanol-ATMACs (C10−C18) were further structurally elucidated by MS/MS characterization and confirmed via a hydrolysis-based transformation experiment. *In silico* toxicokinetic modeling and *in vivo* rat experiments revealed longer elimination half-lives for silanol-ATMACs compared to ATMACs, indicating their bioaccumulation potential. These silanol-ATMACs were mainly detected in medical disinfectants with a median total concentration (∑silanol-ATMAC) of 779 mg/L. While detected at modest levels in indoor dust (median: 8.04 ng/g), silanol-ATMACs exhibited elevated concentrations in human serum, comparable to those of 18 traditional QACs (medians: 10.6 and 13.9 ng/mL, respectively). Our findings demonstrate the application of PA-UF-MS for prioritizing emerging bioaccumulative contaminants and highlight the need for further toxicological evaluation and human exposure assessment of silanol-ATMACs.

KEYWORDS: *quaternary ammonium compounds (QACs), silanol-ATMACs, protein affinity mass spectrometry, human serum albumin (HSA), bioaccumulation, human exposure*

INTRODUCTION

Quaternary ammonium compounds (QACs) are a large group of synthetic chemicals that serve as disinfectants, antimicrobials, and surfactants in various products, including cleaning products, personal care products, pharmaceuticals, pesticides, and biomedical materials.[1] The three most well-known QAC groups are benzylalkyldimethylammonium compounds (BACs, with C8−C18 alkylated chains), dialkyldimethylammonium compounds (DADMACs, with C8−C18 alkylated chains), and alkyltrimethylammonium compounds (ATMACs, with C8−C18 alkylated chains). Since the breakout of the COVID-19 pandemic, the demand for QACs used as antimicrobials has increased substantially.[2] The U.S. Environmental Protection Agency's (EPA) List N has over 200 products containing QACs as active ingredients.[1] Several QACs are high-production

Received: September 29, 2025
Revised: January 28, 2026
Accepted: January 29, 2026

volume chemicals with manufactured or imported amounts exceeding one million pounds per year.[1]

Due to their extensive use in indoor environments, particularly during the COVID-19 pandemic, QACs have become ubiquitous indoors, resulting in widespread human exposure.[3−5] Our previous study confirmed that disinfectant products are a major contributor to QACs in residential dust.[3] Given their presence across multiple exposure pathways, there is increasing concern about their internal exposure and potential bioaccumulation in the human body.[6] Although QACs are generally believed to be rapidly metabolized and excreted via urine and feces as hydroxylated and carboxylated metabolites,[7] their bioaccumulation potential remains controversial. Through an *in vitro*−*in vivo* extrapolation (IVIVE) model, we found that C12-QACs have the highest predicted bioaccumulation potential, with *in vivo* hepatic clearance rates ranging from 0.114 to 2.47 mL/h/g.[6] This aligns with our biomonitoring findings, which revealed the frequent detection of QACs, particularly C12-BAC, in human blood and breast milk with median concentrations of 0.289−0.634 and 0.38 ng/mL, respectively, indicating their potential for accumulation.[8,9] However, only a limited number of QACs have been evaluated for bioaccumulation potential,[10] and few have been monitored in human blood samples.[6,9] Considering the structural diversity of emerging QACs,[4] there is an urgent need for a high-throughput assessment framework to systematically evaluate their bioaccumulative properties and facilitate biomonitoring in human matrices.

Various approaches have been developed to evaluate the bioaccumulation potentials of environmental contaminants, including *in vivo* bioconcentration factor (BCF) tests using fish[11] and octanol−water partition coefficient measurements based on OECD Test Guidelines.[12] However, these conventional methods are often limited by high costs, long duration, and low throughput, making them impractical for screening the vast number of emerging QACs. As a result, the bioaccumulation potential of most QACs remains poorly characterized. Inspired by the strategy of affinity purification with nontarget analysis (APNA), which has been successfully used to identify biologically relevant ligands from complex environmental samples,[13,14] we sought to develop a similar approach to evaluate bioaccumulation potentials of QACs. Our previous study showed that approximately 72−97% of QACs will be bound to serum proteins, demonstrating a strong binding affinity between QACs and serum proteins.[6] Thus, we hypothesized that key plasma proteins in human blood could serve as molecular baits to enrich QACs with greater bioaccumulative potential,[15,16] thereby increasing their likelihood of detection in biomonitoring studies.

To extend our protein-affinity-based approach, we applied ultrafiltration mass spectrometry (UF-MS), a high-throughput technique for ligand screening.[17−23] In addition to its ability to quantify protein−ligand binding affinities,[24,25] similarly to conventional approaches such as isothermal titration calorimetry (ITC), nuclear magnetic resonance (NMR), surface plasmon resonance (SPR), and fluorescence-based techniques, UF-MS further enables efficient screening and identification of unknown small-molecule ligands in complex systems,[17,26] which is difficult to achieve using these traditional methods. However, UF-MS is prone to nonspecific binding on filter membranes, leading to false positives.[27] To address this, we first developed the two-filter UF-MS method to minimize nonspecific interactions and increase identification accuracy. Then, we tested 18 QACs for their binding to three major serum proteins, including human serum albumin (HSA), human liver fatty acid binding protein (hL-FABP), and transthyretin (TTR), which have been reported to be important carriers of endogenous and exogenous compounds.[28−32] Based on these results, we established a protein affinity UF-MS strategy (PA-UF-MS) to screen for high serum transporter protein affinity QAC ligands in disinfectants. Moreover, the bioaccumulation potentials of the newly identified QACs were validated using *in silico* prediction, toxicokinetic modeling with *in vivo* data, and molecular docking analysis. Finally, we quantified a broad range of QAC homologues, including traditional QACs and newly identified QACs in disinfectants, indoor dust, and human serum.

MATERIALS AND METHODS

Chemicals and Reagents

Eighteen QAC native standards were obtained from online reagent companies,[4] a technical standard of silane quaternary ammonium salt (silane-C18-ATMAC) was purchased from Aladdin (Shanghai, China). Three mass-labeled internal standards, including benzyldimethyldodecylammonium-d_7 chloride (d_7-C12-BAC), benzyldimethyltetradecylammonium-d_7 chloride (d_7-C14-BAC), and decyltrimethylammonium-d_9 bromide (d_9-C10-BAC), were purchased from Toronto Research Chemicals (Toronto, ON, Canada). HSA was purchased from HARVEYBIO (Beijing, China), while hL-FABP and TTR were obtained from Sino Biological (Beijing, China). Ultracentrifugal filters (Amicon Ultra-0.5, 10 kDa) were obtained from Millipore Corp (Bedford, MA, U.S.A.). All solvents used in this study were Optima-grade.

Sample Collection and Pretreatment

Seventeen disinfectants from different brands were purchased from JD.com, one of the largest online commercial shopping platforms, between February and March 2023 in China. These disinfectants were manufactured within the past three years, and all of them are frequently used with sales volumes ranked within the top 10 in the Chinese market. For the analysis of disinfectants, 10 μL of a sample was diluted with 9.99 mL of methanol, and then 1 mL of the diluted disinfectants was spiked with the internal standard (d_7-C14-BAC) prior to instrumental analysis.

Thirty-eight dust samples were collected from residential homes in Shenzhen, China, from July to September 2022. The samples were collected using a precleaned nylon stock (with a pore size of 25 μm) coupled with a commercial vacuum cleaner (Dyson, V8 Fluffy Extra). After the nylon bag was detached and wrapped in clean aluminum foil, it was placed in a polypropylene (PP) bag, transported to the laboratory, and stored at −20 °C for further chemical analysis. Briefly, approximately 100 mg of sieved dust was weighed into a polypropylene tube, spiked with surrogate standards (d_7-C12-BAC and d_9-C10-ATMAC), and extracted with 4 mL of acetonitrile using sonication at room temperature. The extraction procedure was repeated in replicates. After extraction, the combined extracts were concentrated to near dryness under a gentle nitrogen stream and then reconstituted in 1 mL of methanol, followed by the addition of the internal standard (d_7-C14-BAC) prior to instrumental analysis.

A total of 90 blood samples were obtained from delivering women recruited through the Third Affiliated Hospital of Sun Yat-sen University from April to July 2019. All participants gave informed consent before participation. The study protocols were approved by the Research Ethics Committee of The Third Affiliated Hospital of Sun Yat-sen University ([2019]02-637-01) and the Research Ethics Committee of Jinan University (JUNKY-2021-011). Each blood sample was immediately centrifuged at 3000 rpm for 5 min at 4 °C to collect serum. HPLC water was also collected into the same type of tubes as field blanks, along with blood collection. Serum samples were stored at −80 °C until chemical analysis.

Serum sample pretreatment was processed according to previous methods with a minor modification.[33,34] Briefly, 200 μL of serum samples, thawed at room temperature, were fortified with the surrogate

https://doi.org/10.1021/acs.est.5c13764
Environ. Sci. Technol. XXXX, XXX, XXX−XXX

standards (d_7-C12-BAC) and were extracted in 3 mL of ethyl acetate with a multi-tube vortexer for 20 min. The sample was then centrifuged at 3500 rpm for 5 min, and the supernatant was transferred to a new tube. This re-extraction process was repeated twice more, for a total of three extractions, and the supernatants were combined. The extract was further evaporated to dryness and reconstituted in 50 μL of methanol and frozen at −80 °C overnight. Following centrifugation at 15000 rpm for 5 min, the supernatant was collected and spiked with the internal standard (d_7-C14-BAC) prior to instrumental analysis.

Development of the Ultrafiltration Mass Spectrometry (UF-MS) Method

Mixtures of C12-QACs (C12-BAC, C12-DADMAC, and C12-ATMAC) and C14-QACs (C14-BAC, C14-DADMAC, and C14-ATMAC) were selected as the substrate to evaluate the effectiveness of the UF-MS method in reducing nonspecific binding. For one filter procedure, the final reaction mixtures consisted of 199 μL of HSA (7.5 μM) in 0.1 M phosphate buffer saline (PBS) solution (pH 7.4) and 1 μL of substrate (0.5 μM) in dimethyl sulfoxide (DMSO). Incubations were carried out in triplicate in 2 mL centrifuge tubes at 37 °C, and 150 μL was transferred to an ultrafiltration device (Millipore, 10 kDa) after 60 min. 200 μL 0.1 M PBS solution (pH 7.4) was added into each ultrafiltration device before 10 min centrifugation (13 000 rpm at 4 °C) was carried out, and repeated three times to eliminate unbound ligands. After the washing step, 200 μL of ice-cold acetonitrile was added to each ultrafiltration device, and then it was centrifuged at 13 000 rpm for 20 min at 25 °C. The final total volume of 600 μL was prepared for further chemical analysis. The process was repeated twice to disrupt the protein−ligand complexes.

For the two-filter procedure, samples were prepared similarly to those in the one-filter procedure. In order to minimize the extent of nonspecific binding, a new filter was substituted for the ultrafiltration filter prior to the ligand dissociation and elution step (Figure S1).[35] Incubations containing no protein were used as control samples to assess potential nonspecific binding (NSB) interference.

HSA, hL-FABP, and TTR (7.5 μM for each) were selected to identify the protein with the highest bound fraction toward QACs. The two-filter procedure was employed on a mixture of 18 QACs (0.5 μM for each QAC), including C8−C18 BACs, C8−C18 DADMACs, and C8−C18 ATMACs. All steps were performed as previously described, except for the solution used for hL-FABP, which was dissolved in 50 mM Tris−HCl, 150 mM NaCl, and 1 mM dithiothreitol (pH 8.0).

All final solutions were spiked with an internal standard (d_7-C14-BAC) before instrumental analysis. The NSB of QACs to the ultracentrifugal filter and the bound fraction of QACs to serum protein (f_b), reflecting their relative binding affinities, were measured using the equations below[36,37]

$$\mathrm{NSB} = 1 - \frac{M_{\mathrm{after}}}{M_{\mathrm{before}}} \quad (1)$$

$$f_b = \frac{M_b}{M_t} \times 100\% \quad (2)$$

where M_{after} is the molar mass of QACs in the buffer after centrifugation, M_{before} is the molar mass of QACs in the buffer before centrifugation, M_b is the molar mass of the bound compound, and M_t is the initial molar mass of the compound.

Protein Affinity Pull-Down Using the Two-Filter Ultrafiltration Mass Spectrometry

To prepare the mixed disinfection product solution, equal aliquots (20 μL each) of the individual disinfection products (n = 17) were diluted 100-fold and combined to achieve a standardized cocktail for subsequent binding experiments. One μL of the cocktail solution was incubated with 199 μL of HSA solution (50 μM) in 0.1 M PBS (pH 7.4). The incubation, ultrafiltration, and pretreatment methods were performed as described in the previous section. Oleic acid, an endogenous ligand of HSA, was included as a positive control to confirm the effectiveness of the pull-down assay.

The nontarget analysis was conducted using an Agilent 1290 Infinity ultrahigh-performance liquid chromatograph system coupled to an Agilent 6546 quadrupole time-of-flight mass spectrometer (UPLC-QTOF/MS) (Santa Clara, CA) in electrospray ionization positive mode (ESI+). Details of the instrumental methods are presented in Text S1. To identify the potential QACs binding to HSA through the PA-UF-MS strategy, a suspect list of more than 200 QACs was included in the in-house database established in our previous study.[4] The data analysis workflow was performed as follows: the high-resolution mass spectrometry (HRMS) raw data were converted to mzXML format and deconvolved by XCMS online for feature detection, filtering, and alignment across samples. Formula assignment and suspect screening were performed in Agilent MassHunter qualitative software (version B.10.1). In detail, formula assignment was predicted using an elemental composition range of $C_{0-50}H_{0-200}N_{0-3}O_{0-10}P_{0-10}S_{0-10}Si_{0-10}$ with a mass error of 5 parts per million (ppm). Suspect screening was performed with the Molecular Feature Extraction (MFE) algorithm (peak height >600 counts; $[M]^+$ adducts), which matched to theoretical exact mass (<5 ppm) and retention times (<0.2 min) of the in-house database, and were further incorporated into the MS/MS preferred list. Features not matched with our in-house database but with a high score (>95) and containing heteroatoms (O, P, S, and Si) were prioritized for obtaining their MS/MS spectra. For the structure elucidation of the features, MS/MS spectra were confirmed using commercial standards or compared with MS information in public libraries (i.e., mzCloud and MassBank). Moreover, a synthesized standard of silanol-C18-ATMAC was used to confirm its tentative structure, which was prepared through a simple hydrolysis reaction by mixing silane-C18-ATMAC with pure water for 60 min. A detailed procedure is provided in Text S2.

For ligand annotation, identification confidence was reported using the Schymanski classification,[38] with level 1 (confirmed by standards), level 2 (probable structures supported by MS/MS evidence or library matching), and level 3 (tentative candidates without unique structural confirmation).

Pseudotargeted Analysis of Silanol-ATMACs in Human Blood Using HPLC−MS/MS

Pseudotargeted analysis was employed to enhance the sensitivity of detection and reduce false positives in the quantification of silanol-ATMACs within complex serum matrices.[39] Instrumental analysis was performed on an ultraperformance liquid chromatograph coupled to a 5500 Q Trap triple quadrupole mass spectrometer (AB Sciex, Toronto, ON) in positive electrospray ionization (ESI+) mode. Separation of the target analytes was performed on an Acquity UPLC RP C18 column (100 mm, 2.1 mm i.d., 1.7 μm thickness, Waters). The mobile phase consisted of water with 5 mM ammonium acetate (A) and acetonitrile (B), both containing 0.1% formic acid. The flow rate was maintained at 0.4 mL/min. The gradient used was as follows: 5% B for the initial 1.5 min, increased to 50% B by 4.5 min, followed by an increase to 100% B at 10 min and held for 5 min, then returned to 5% B at 15.1 min, and equilibrated for 2 min after each run. The injection volume was set to 5 μL. The settings for the nebulizer, gas flow, gas temperature, capillary voltage, sheath gas temperature, and sheath gas flow were 25 psi, 10 L/min, 300 °C, 3500 V, 350 °C, and 12 L/min, respectively. Data acquisition was conducted in a multiple reaction monitoring (MRM) mode, with the optimized MRM transitions, declustering potential, and collision energies detailed in Table S1.

(Semi-)Quantification of Silanol-ATMACs

Quantification of target analytes was performed using extract mass (±5 ppm) extracted ion chromatograms (EICs) from full scan measurements. For 18 traditional QACs, the quantification of these analytes using commercial standards was conducted via isotope dilution based on a linear internal regression calibration curve. For 5 newly identified silanol-ATMACs lacking commercial standards, given their structural similarity to ATMACs, semi-quantification was performed by assuming the silanol-ATMACs have equal molar instrumental responses compared to the reference standard of ATMACs. Both (semi-

https://doi.org/10.1021/acs.est.5c13764
Environ. Sci. Technol. XXXX, XXX, XXX−XXX

)quantification using a linear regression calibration ranging from 1 to 100 ng/g with regression coefficients of >0.99.

In Silico Bioaccumulation Potential Assessment

The half-lives of silanol-ATMACs and ATMACs were estimated using the online bioaccumulation prediction platform (http://tkpara.hhra.net), which is built upon a stacking machine learning framework that integrates multiple base learners and is optimized via linear regression techniques. The model was trained on a curated data set of 2934 chemicals with experimentally derived human half-life values. All compounds were entered in SMILES format, and molecular descriptors were automatically extracted and processed within the platform to generate predictions relevant to pharmacokinetic behavior.

In Vivo Bioaccumulation Potentials Assessment of Silanol-C18-ATMAC and C18-ATMAC

Six-week-old Sprague−Dawley rats (three males and three females, 155 ± 5 g) were purchased from Weitong Lihua (Beijing, China). All animal procedures were approved by the Animal Use and Care Committee of Shenzhen Huateng Biomedical Technology Co., Ltd. (Protocol B202409-1). Rats were housed under standard conditions (12 h light−dark cycle, 22 ± 2 °C, 50 ± 10% relative humidity). Due to the absence of an authentic silanol-C18-ATMAC standard, we prepared a stock solution by mixing several commercial products. The mixing ratios were determined based on the weighted average concentrations of C18-ATMAC and silanol-C18-ATMAC present in each product. Consequently, C18-ATMAC and silanol-ATMACs were administered via intravenous injection at equal doses of 0.1 mg/kg. It should be noteworthy that the administered doses were below the known LD_{50}. The formulation of this stock solution, administered doses, and reported LD_{50} values are presented in Table S2. Blood was collected from the tail vein at 0, 0.2, 0.5, 1, 1.5, 2, 4, and 8 h into polypropylene tubes and stored at −80 °C.

A 100 μL aliquot was extracted with 0.4 mL of acetonitrile using sonication for 30 min, centrifuged at 8000 rpm for 10 min, and the procedure was repeated twice. The combined supernatant was filtered (0.2 μm nylon), spiked with d_7-C14-BAC as an internal standard before instrumental analysis. The half-life of the target analyte in blood was determined using the one-phase exponential decay function in GraphPad Prism (version 9.0.0).[40,41]

Molecular Docking

The 3D structures of C18-ATMAC and silanol-C18-ATMAC were drawn in ChemDraw and converted to energy-minimized 3D conformations with Chem3D. Molecular docking was performed using AutoDock Vina (v1.2.7)[42] to evaluate the binding affinity of both compounds with HSA (PDB: 1H9Z),[43] focusing on Sudlow sites I and II as potential QAC-binding sites.[44−46] Protein structures were preprocessed by removing water molecules and native ligands. Ligands were prepared with AutoDockTools (v1.5.7), and the top 9 ranked docking scores were evaluated based on conformations, orientations, and binding energies. The top-ranked docking poses were visualized using PyMOL (v2.4.0), and protein−ligand interactions were further analyzed in Discovery Studio. Detailed docking parameters are provided in Text S3.

Isothermal Titration Calorimetry Titrations

The Microcal VP-ITC (MicroCal, LLC, Northampton, MA, U.S.A.) titrator was used for the calorimetric titrations. The HSA and four QACs (CPC, C14-ATMAC, C12-BAC, and C10-DADMAC) solutions were prepared with PBS buffer (pH 7.4). HSA solutions were 0.05 mM, and the concentration of QACs solutions ranged from 0.5 to 1.42 mM. The titrations were performed at 25 °C. The injection volume was 10 μL and the interval between injections was 120 s to guarantee the equilibrium in each titration point. The obtained data were analyzed through the Origin 7.0 software supplied by Microcal. The ITC data were collected automatically and analyzed to get the binding site number (n), the dissociation constant (K_d), the enthalpy change (ΔH), and the entropy change (ΔS) associated with the interaction.

Quality Assurance and Quality Control (QA/QC)

Acetonitrile extraction recoveries for the 18 QACs in the protein−ligand incubation solution ranged from 77 to 97% (with the exception of C16-ATMAC, 64%), while matrix effects were minimal, ranging from 96 to 105% (Tables S3 and S4). QACs concentrations in dust and serum were corrected by subtraction of the procedural blank levels from the sample levels. Method detection limits (MDLs) were set as 3 times the standard deviation of target analyte levels detected in the procedural blanks. For compounds not detected in the procedural blanks, MDLs were defined as the analyte concentrations corresponding to a signal-to-noise ratio of three. MDLs, procedural blanks, and field blanks for all target analytes are included in Table S5. The recoveries of BACs, DADMACs, and ATMACs ranged from 93 to 108%, from 77 to 104%, and from 104 to 134% for dust and from 91 to 106%, from 61 to 136%, and from 101 to 119% for serum, respectively (see the complete data in Table S6).

Data Analysis

Basic and descriptive statistics were conducted using IBM SPSS Statistics 24 and Microsoft Excel 2021. A Mann−Whitney test was used for the comparison of the logarithmically transformed concentrations. Differences between groups for the peak features pulled out were compared by Student's t test. The difference was considered statistically significant at a p value of <0.05.

RESULTS AND DISCUSSION

Method Development of Ultrafiltration Mass Spectrometry

QACs are readily adsorbed onto container surfaces due to their unique cationic properties, which may lead to strong nonspecific binding of QACs to the filters.[47] As shown in Figure S1, all tested QACs, including C12- and C14-BACs, C12- and C14-DADMACs, and C12- and C14-ATMACs, exhibited high NSB in the one-filter UF−MS procedure (21 ± 3 to 105 ± 16%), rendering this approach unsuitable for quantifying their binding affinities to serum proteins. After adopting the two-filter procedure previously used to eliminate NSB in retinoic acid receptor ligand screening,[48] the NSB of C12-QACs and C14-QACs was substantially reduced to 0.516−14.3%. These results demonstrated that the two-filter UF-MS procedure has the potential to decrease the NSB of QACs.

To identify the primary protein contributors to QAC binding in blood, we evaluated the bound fractions of 18 commonly used QACs with three representative transport proteins, including HSA, hL-FABP, and TTR. In general, QACs exhibited the strongest binding affinities toward HSA with f_b ranging from 0.37 to 99.9%, significantly higher than those for hL-FABP and TTR (from 0.01 to 10.3% and from 0.85 to 46.0%, respectively; Figure S2). This is likely due to HSA's unique structure, which includes two main binding sites and several additional hydrophobic pockets,[49,50] and numerous nonspecific binding sites on the surface, enabling broad ligand interactions.[51] A similarly wide range of f_b has been reported for methylimidazolium chlorides with C4−C12 alkyl chains, where no binding was observed for C4, while C12 reached up to 85%.[52] The weak binding of short-chain QACs to HSA is likely due to insufficient van der Waals interactions within the binding sites.[53] This result suggests that HSA may serve as a more significant binding protein for QACs in blood than hL-FABP and TTR. Based on this rationale, HSA was selected as the primary target protein for subsequent PA-UF-MS analysis.

Interestingly, the f_b generally increased with the alkyl chain for the C8−C16 compounds, then declined for the C16−C18 QACs in the case of HSA. By contrast, neither hL-FABP nor TTR exhibited a consistent trend in bound fractions comparable to that observed for HSA. For hL-FABP, binding was

https://doi.org/10.1021/acs.est.5c13764
Environ. Sci. Technol. XXXX, XXX, XXX−XXX

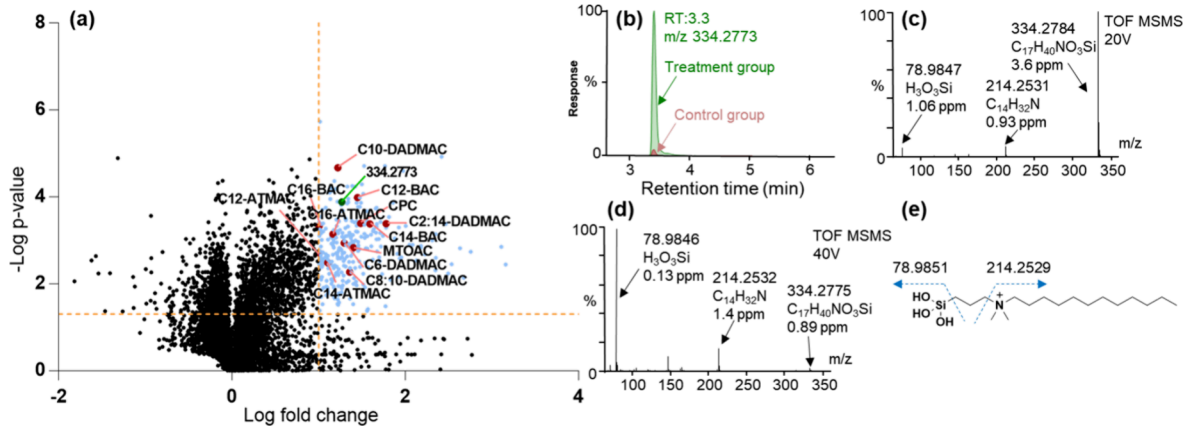

Figure 1. Identification of HSA ligands in the mixtures of commercial disinfectants by PA-UF-MS strategy. (a) Volcano plots representing the log-transformed fold changes (FCs) and corresponding p values of each feature measured in the mixtures of commercial disinfectants. Blue dots represent the features that have conspicuously abundant abundances (FCs > 10; $p < 0.05$), while red dots represent the identified compounds from pulled-out features. (b) Comparison of the representative LC chromatograms of the identified pulled-out features detected in treatment groups and control groups. (c and d) Corresponding MS/MS spectrum of the identified pulled out features of panel b detected in the mixtures of commercial disinfectants under different collision energies. (e) Proposed structure of the identified pulled-out features at m/z 334.2773.

consistently low across all QACs, but a weak parabolic trend with a peak at intermediate chain lengths (C14) was still observable for DADMACs and C10 for ATMACs. For TTR, binding showed a pronounced maximum at C12−C16 specifically for DADMACs, while exhibiting a clear increasing trend with longer chains for both BACs and ATMACs. These differences highlight HSA's more binding sites compared to the more selective and lower affinity hL-FABP and TTR.[51] The strongest HSA binding affinities were observed for C16-QACs, with f_b of 80.8, 99.9, and 68.6% for C16-BAC, C16-DADMAC, and C16-ATMAC, respectively. The structure-dependent binding potency of these compounds can be attributed to a protein−molecular interaction mechanism, in which an optimal chain length facilitates favorable hydrophobic interactions within the HSA's binding pockets.[54,55] It should also be noted that protein−ligand binding affinity is not determined solely by the chemical structure or lipophilicity of the ligand; intrinsic properties of the protein, such as binding pocket geometry, steric compatibility, and specific interaction sites, also play a critical role. Therefore, the observed binding pattern likely reflects the combined influence of both ligand structure and protein binding characteristics.[56] In our previous study, the highest binding affinities to whole human serum were observed for C12-QACs, likely due to the combined contributions of multiple serum proteins that may exhibit complementary binding preferences for this chain length.[6]

Suspect Screening of HSA Ligands in Disinfectants

We then employed the PA-UF-MS strategy to identify potential HSA ligands from commercial disinfectants (Figure S3). Only chemicals exhibiting at least 10-fold higher abundance in the dosed group compared to the negative control group (without protein addition) were considered potential HSA ligands. The effectiveness of the pull-down assay was validated using oleic acid, a positive chemical for HSA, with a FC of 14.3 (Figure S4).

Among the 15 355 features detected under ESI+, 285 features were identified as putative HSA ligands (Figure 1). To annotate these putative ligands, we searched against an in-house database established in our previous studies, which included over 200 QACs reported in the literature.[4] As a result, 12 QACs were tentatively identified in the present study, comprising 8 traditional QACs, including C12-, C14-, and C16-BACs, C6- and C10-DADMACs, and C12-, C14-, and C16-ATMACs, as well as 4 emerging QACs, including cetylpyridinium chloride (CPC), C2:14-DADMAC, C8:10-DADMAC, and methyltrioctylammonium chloride (MTOAC). The identities of these QACs were further confirmed by their corresponding commercial reference standards and previous records (Figure 1 and Figure S5).[4]

Apparently, C12-, C14-, and C16-BACs were identified as high-affinity HSA ligands with FCs of 28.0, 39.0, and 10.1, respectively. Their strong serum protein binding affinity has been reported in our earlier study.[6] CPC, an isomer of C12-BAC, was also identified as a high binding affinity HSA ligand (FC: 30.6), which is reported to be an ingredient in antimicrobial mouthwashes and toothpaste.[10] In addition, C2:14-DADMAC was identified as the most abundant QAC with high HSA-binding affinity (FC: 60.0). Other mixed DADMACs, such as C8:10-DADMAC, were also isolated as putative HSA ligands with a higher FC of 22.9. The binding affinities of these mixed DADMACs were generally higher than those of paired chain DADMACs, including C6-DADMAC and C10-DADMAC (FC: 19.7 and 16.6, respectively). A plausible explanation is that paired-chain DADMACs exhibit greater steric hindrance than mixed-chain DADMACs due to their structural symmetry and increased bulk near the pharmacophore, which may restrict favorable electrostatic and hydrophobic interactions with HSA.[57] Nevertheless, further investigation is warranted to confirm the observed higher FCs of mixed-chain DADMACs. In addition, most ATMACs, including C12-ATMAC, C14-ATMAC, and C16-ATMAC, were isolated as putative HSA ligands with FCs of 10.1, 12.7, and 14.7, respectively. The binding affinities of ATMACs to HSA were comparable to those of paired chain DADMACs (FCs: 16.6−19.7), which were generally lower than those of BACs (FC: 10.1−39.0). Furthermore, MTOAC, a structural analogue of ATMACs, was identified as a high-affinity HSA ligand with a higher FC of 25.3, even higher than those of traditional ATMACs discussed above. Overall, these results demonstrate a structure-dependent binding affinity of QACs to HSA.

Among the identified high-affinity HSA ligands, only C12-BAC, C14-BAC, C12-ATMAC, C14-ATMAC, and C16-ATMAC have demonstrated bioaccumulation potential and

https://doi.org/10.1021/acs.est.5c13764
Environ. Sci. Technol. XXXX, XXX, XXX−XXX

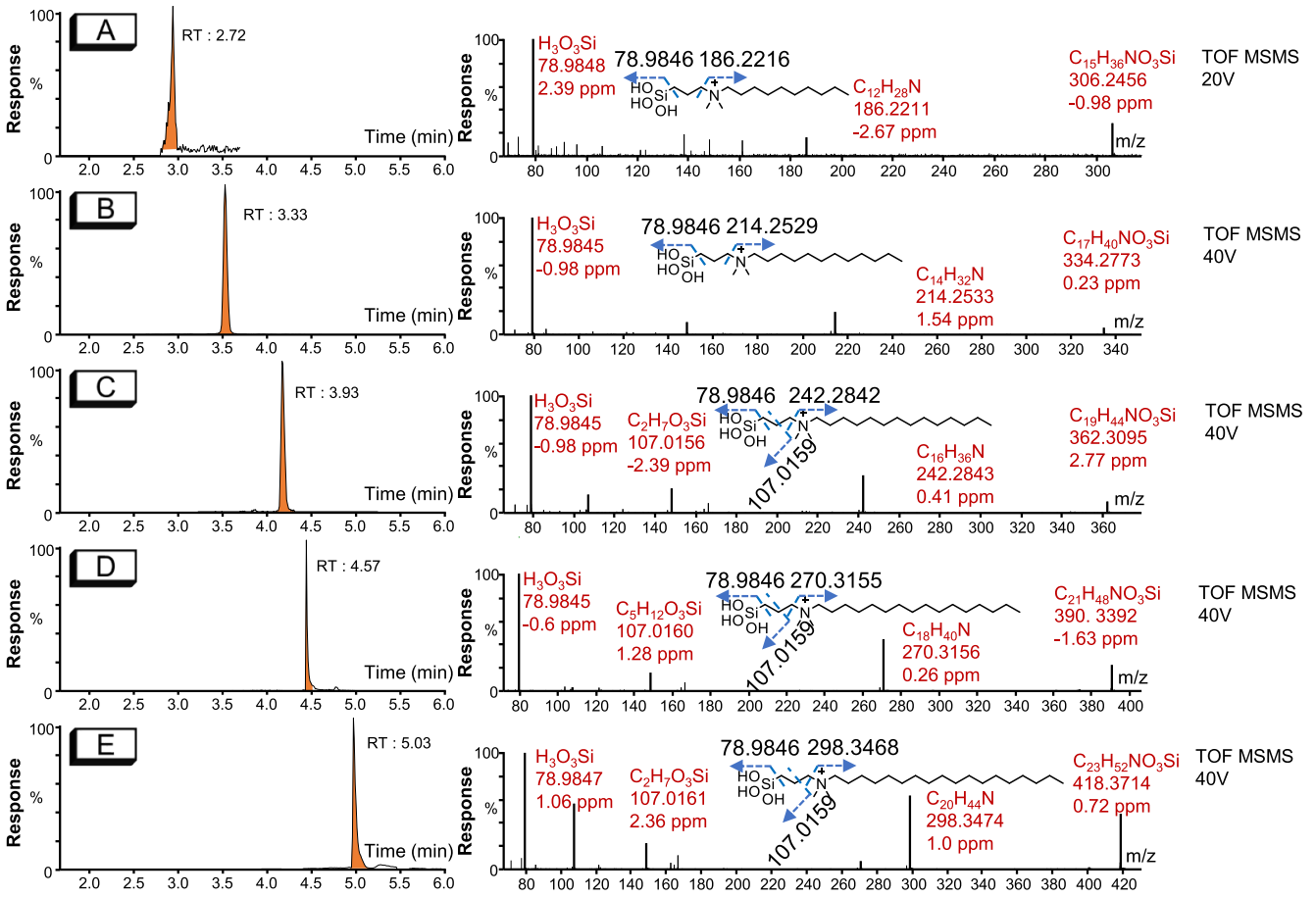

Figure 2. LC-TOF-MS chromatograms and MS/MS spectra of silanol-ATMACs detected in disinfectants. (a−e) Silanol-C10-ATMAC (RT of 2.72 min), silanol-C12-ATMAC (RT of 3.33 min), silanol-C14-ATMAC (RT of 3.93 min), silanol-C16-ATMAC (RT of 4.57 min), and silanol-C18-ATMAC (RT of 5.03 min).

have been detected in human serum.[4] However, for the other newly identified QACs, a more comprehensive assessment of their bioaccumulation potency and biomonitoring is warranted in the future, particularly for those not routinely measured in human blood.

Comparison between the Bound Fraction and ITC Parameters

To further validate whether the FC obtained from the pull-down assay, which serves as a relative measure of the bound fraction, reliably reflects the binding affinity of compounds to HSA, supplementary ITC experiments were conducted on four representative QACs (C12-BAC, C14-ATMAC, CPC, and C10-DADMAC) that exhibited distinct fold change values (12.7−30.6) in the pull-down assay.

As shown in Table S7 and Figure S6, for three compounds with comparable binding site numbers (n), namely, CPC (n = 1.64), C12-BAC (n = 1.94) and C14-ATMAC (n = 1.13), the trend of fold change values derived from the pull-down assay were in good agreement with their ITC-derived K_d values, with lower K_d corresponding to higher FC. ITC analysis further revealed that the binding of these three compounds to HSA was characterized by negative enthalpy changes ($\Delta H < 0$) and positive entropy changes ($\Delta S > 0$), resulting in negative Gibbs free energy changes ($\Delta G < 0$), indicative of spontaneous binding.[58,59]

In contrast, C10-DADMAC exhibited a higher FC than C14-ATMAC despite having a weaker binding affinity (higher K_d). This apparent discrepancy can be attributed to its significantly larger binding site numbers (n = 8.7), which contribute to a higher overall bound fraction. Notably, the interaction between C10-DADMAC and HSA was endothermic, with both ΔH and ΔS being positive. It suggests that the binding process is predominantly driven by hydrophobic interactions. Moreover, the Gibbs free energy change calculated using the van't Hoff equation ($\Delta G = \Delta H - T\Delta S$) was negative (−5.71 kcal/mol), confirming that the binding of C10-DADMAC to HSA is also spontaneous.[60]

Taken together, these results demonstrate that the FC obtained from the pull-down assay can effectively represent the relative binding affinity of compounds to HSA. However, because FC is jointly determined by K_d and n,[61] FC does not provide quantitative thermodynamic parameters. Therefore, quantitative techniques such as ITC are necessary for mechanistic interpretation and precise affinity determination.

Nontarget Screening of HSA Ligands in Disinfectants

Among the 285 putative ligands captured by the HSA proteins, only 12 features matched entries in the suspect screening list (Table S8). The majority of statistically significant features (p < 0.05) exhibiting high FCs over 10 remained unidentified. Therefore, we then moved forward to elucidate the structures of other potential emerging QACs with high bioaccumulation potentials through nontarget analysis. In general, traditional QACs typically consist only of C, H, and N atoms and account for 1−3% (w/w) in disinfectant formulations. To better account

https://doi.org/10.1021/acs.est.5c13764
Environ. Sci. Technol. XXXX, XXX, XXX−XXX

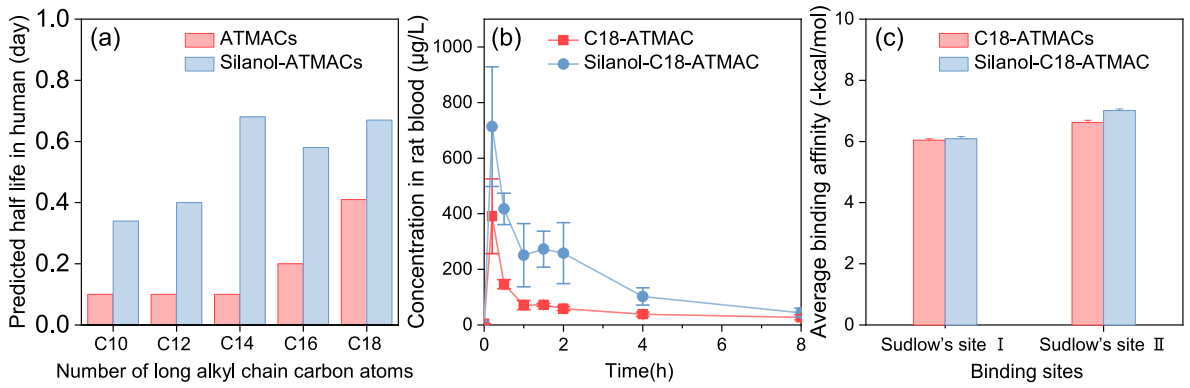

Figure 3. Bioaccumulation potentials assessment of silanol-ATMACs (blue) and ATMACs (red). (a) Predicted half-life in human (days) by chain length (C10−C18). (b) Concentration in rat blood (μg/L) over 8 h post-dose (mean ± SD; $n \geq 3$). (c) Average binding affinity (−kcal/mol) at Sudlow's site I and Sudlow's site II of human serum albumin (HSA) (−kcal/mol; higher values indicate stronger binding).

for the unidentified features, we broadened our formula search to include heteroatoms such as Si, P, and S, which are frequently incorporated into commercial products to enhance specific functional properties.[62,63] We used MassHunter qualitative analysis to predict molecular formulas and calculate ring and double bond equivalents (RDB) for the unknown features, using a broad elemental composition range ($C_{0-100}H_{0-100}O_{0-50}N_{0-50}Si_{0-10}P_{0-10}S_{0-10}$). Among the predicted candidates, one molecular ion with the formula $C_{17}H_{40}NO_3Si$, containing both silicon and nitrogen, was not found in our in-house database. This feature showed a high intensity in the full scan MS^1 spectrum and exhibited a FC of 18.5 ($p < 0.05$), warranting further structural characterization. To elucidate its potential structure, the precursor ion of m/z 334.2773 was included in the data-dependent acquisition (DDA) preferred list for HRMS acquisition to obtain its MS/MS spectra at stepwise collision energies (20 and 40 eV). For example, a collision energy of 20 eV produced fragments that included m/z 78.9846 ($H_3O_3Si^+$, 0.13 ppm), indicative of a silanol group, and m/z 214.2532 ($C_{14}H_{32}N^+$, 1.4 ppm), supporting the presence of a quaternary ammonium structure. To further confirm the structure, an online search using the elemental formula yielded a match in the PubChem database with compound CID of 154153066 (dodecyl-dimethyl-(3-trihydroxysilylpropyl)azanium (CAS number: not available). Collectively, the candidate was identified as silanol-C12-ATMAC, which was a structural analogue of C12-ATMAC.

Next, we proceeded to directly extract peaks with diagnostic fragment ion (m/z 78.9846, $H_3O_3Si^+$) to search for potential silanol-ATMAC candidates in crude disinfectants. Consequently, in addition to silanol-C12-ATMAC, a series of silanol-ATMAC homologues with varying carbon chain lengths, including silanol-C10-ATMAC, silanol-C14-ATMAC, silanol-C16-ATMAC, and silanol-C18-ATMAC, were also identified in these products. The identities of these silanol-ATMACs were further evidenced by their stepwise retention times with increasing carbon chain lengths and identical fragmentation patterns (Figure 2 and Figure S7). Notably, silanol-C14-ATMAC, silanol-C16-ATMAC, and silanol-C18-ATMAC were observed to be significantly pulled out by HSA protein ($p < 0.05$) but with relatively low FCs of 4.71, 3.35, and 2.61, respectively.

No authentic standards were available to further validate the identification of these silanol-ATMACs. Fortunately, we found a commercial standard available under the name of (3-(trimethoxysilyl)propyl)octadecyldimethylammonium (silane-C18-ATMAC), a structural analogue of silanol-C18-ATMAC, which is mainly used as an antibacterial agent in household products.[64] Previous studies have demonstrated that silane groups readily hydrolyze to silanol in the presence of water.[65,66] Therefore, silane-ATMACs composed of silane coupled to a QAC structure are expected to undergo the same hydrolytic transformation as other silanes. To further validate this potential transformation pathway of silane-C18-ATMAC, a laboratory hydrolysis experiment was conducted in an aqueous solution. As a result, an increasing trend in silanol-C18-ATMAC concentration was observed, accompanied by a decrease in silane-C18-ATMAC levels, followed by stabilization after 60 min (Figure S8). Subsequently, we analyzed the mixture solution prepared in our study using the same LC conditions and DDA mode as those used for disinfectants. The extracted ion chromatograph of m/z 418.3714 ($C_{23}H_{52}NO_3Si^+$, 0.72 ppm) in the full scan spectrum of the mixture solution exhibited the same retention time as that in disinfectants (Figure S9). This was further evidenced by the characteristic fragment ion m/z 78.9847 ($H_3O_3Si^+$, 1.06 ppm) and m/z 298.3474 ($C_{20}H_{44}N^+$, 1.0 ppm) in their MS/MS spectra, observed in the mixture solution and consistent with those of disinfectants (Figure S9).

To the best of our knowledge, these silanol-ATMACs were first developed by Dow Corning Corp. (Midland, MI) under the trade name of 5700 Antimicrobial Agent (DC 5700) as early as 1967, which were designed to fulfill antibacterial functions in textiles.[67] In addition to these early applications, silanol-ATMACs have been patented and utilized as solvent-free or water-stable compositions for cleaning hard and soft surfaces, including office furnishings and healthcare facility coatings, where they provide durable antimicrobial protection through covalent bonding to substrates.[68−70] Beyond surface cleaning, they have also been employed as emulsifiers or shampoo conditioners, surfactants, and flocculants in softeners, consumer products, pesticides, and wastewater treatments.[71−74] More recently, silanol-ATMACs have been formulated into alcohol-free or biocompatible systems to provide long-lasting antimicrobial activity in medical and personal care applications, including oral sterilization, wound disinfection, intracanal medicaments in dentistry, and antiherpesviral treatments.[75] Given their widespread usage across diverse environments and applications, it is important to understand their presence and distribution in both environmental and biological matrices.

https://doi.org/10.1021/acs.est.5c13764
Environ. Sci. Technol. XXXX, XXX, XXX−XXX

Table 1. Confidence Level (CL), Detection Frequencies (DF, %), Median Concentrations, and Contribution of Each QAC (Contr, %) Measured in Household Disinfectants (mg/L), Medical Disinfectants (mg/L), Residential Dust (μg/g), and Human Serum (ng/mL)[a]

		household disinfectants			medical disinfectants			residential dust			serum		
compound	CL	DF	median	contr	DF	median	contr	DF	median	contr	DF	median	contr
						BACs							
C8-BAC	L1	100	0.161	0.0115	71	0.208	0.253	97	0.037	0.121	8		
C10-BAC	L1	90	2.74	0.195	43	2.89	3.52	100	0.0914	0.298	30		
C12-BAC	L1	100	856	60.8	100	3.30	4.02	100	14.3	46.8	100	0.827	7.1
C14-BAC	L1	100	305	21.7	100	1.44	1.76	100	5.24	17.1	100	0.770	6.61
C16-BAC	L1	100	9.82	0.698	100	4.01	4.88	100	0.335	1.09	78	0.258	2.21
C18-BAC	L1	100	11.8	0.839	86	13.4	16.3	100	0.289	0.943	24		
						DADMACs							
C8-DADMAC	L1	60	24.4	1.73	29	3.49	4.26	100	0.135	0.441	2		
C10-DADMAC	L1	100	159	11.3	100	0.887	1.08	100	0.463	1.51	99	1.91	16.4
C12-DADMAC	L1	100	0.407	0.029	100	0.197	0.24	97	0.0283	0.0924	3		
C14-DADMAC	L1	100	0.04	0.00284	100	0.0438	0.0534	100	0.0365	0.119	3		
C16-DADMAC	L1	100	0.293	0.0209	100	0.384	0.468	100	0.34	1.11	58	0.236	2.03
C18-DADMAC	L1	90	1.48	0.106	86	5.58	6.8	100	0.776	2.53	51	0.252	2.16
						ATMACs							
C8-ATMAC	L1	100	0.07	0.00497	100	0.0382	0.0465	87	0.0169	0.055	98	0.113	0.968
C10-ATMAC	L1	100	5.41	0.385	100	0.642	0.782	100	0.0796	0.259	82	0.027	0.232
C12-ATMAC	L1	100	4.36	0.31	100	4.62	5.63	100	1.03	3.36	61	0.231	1.98
C14-ATMAC	L1	100	0.588	0.0418	100	0.95	1.16	100	0.254	0.829	100	1.47	12.6
C16-ATMAC	L1	100	0.584	0.0416	100	6.38	7.77	100	2.0	6.52	100	1.88	16.2
C18-ATMAC	L1	100	24.2	1.72	100	33.6	41	100	5.16	16.8	100	3.67	31.5
						Silanol-ATMACs							
silanol-C10-ATMAC	L3	0			71	5.64	2.07	82	0.00178	25.9	99	1.18	11.8
silanol-C12-ATMAC	L3	0			100	92.4	33.9	87	0.00209	30.3	88	2.65	26.6
silanol-C14-ATMAC	L3	0			100	3.68	1.35	37			91	0.102	1.02
silanol-C16-ATMAC	L3	20	0.723	13.6	100	43.6	16	47			100	3.56	35.8
silanol-C18-ATMAC	L1	100	4.58	86.4	100	127	46.7	50	0.00302	43.8	98	2.46	24.7
∑BAC		100	1180	84.2	100	15.5	1.57	100	19.0	57.1	100	1.94	8.56
∑DADMAC		100	169	12.1	86	15.0	1.53	100	3.54	10.6	100	2.16	9.54
∑ATMAC		100	47.4	3.40	100	175	17.8	100	10.7	32.2	100	7.96	35.2
∑traditional QAC		100	1740	99.7	100	1370	20.9	100	35.9	99.9	100	13.9	53.3
∑silanol-ATMAC		100	4.58	0.30	100	779	79.1	100	0.00804	0.10	100	10.6	46.7
∑QAC		100	1950	100	100	3680	100	100	35.9	100	100	24.5	100

[a]Semi-quantification was performed for silanol-ATMACs.

https://doi.org/10.1021/acs.est.5c13764
Environ. Sci. Technol. XXXX, XXX, XXX−XXX

In Silico and *In Vivo* Bioaccumulation Potential Assessment of Silanol-ATMACs

The predicted half-lives of both silanol-ATMACs and ATMACs increased with increasing alkyl chain lengths (Figure 3a), likely due to enhanced hydrophobicity, which in turn contributes to higher bioaccumulation potential.[6] However, predicted half-lives of silanol-ATMACs did not exhibit a consistently increasing trend with longer alkyl chain lengths, this deviation from the expected chain-length-dependent trend may result from error amplification within the stacked ensemble prediction model, as minor fluctuations from individual base learners can be magnified during model integration.[76] Notably, silanol-ATMACs consistently exhibited longer half-lives than their nonhydroxylated counterparts, suggesting that the introduction of a silanol group significantly enhances their persistence in the human body. This enhancement can be attributed to silicon's role as a bioisostere, which increases molecular lipophilicity (e.g., via larger bond lengths and reduced electronegativity compared to carbon), thereby improving membrane penetration and reducing metabolic clearance across cell barriers.[77] This trend was further validated by *in vivo* bioaccumulation assessment of the available C18-ATMAC and hydrolytically generated silanol-C18-ATMAC (Figure 3b). Silanol-C18-ATMAC persisted in rat blood at higher concentrations for a longer duration compared to C18-ATMAC (half-lives: 0.551 and 0.171 h, respectively), indicating slower systemic clearance. The elevated bioaccumulation potential of silanol-C18-ATMAC is likely due to its stronger binding affinity toward HSA. Due to the limited availability of silanol-ATMAC analytical standards, cross-validation between predicted and experimental half-lives is currently not feasible.

For molecular docking method validation, redocking of the native ligands was performed, and the Root Mean Square Deviation (RMSD) values between the redocked poses and their crystallographic conformations were 0.362 Å for R-warfarin at Sudlow's site I and 1.672 Å for myristic acid at Sudlow's site II, indicating that the docking protocol is reliable. The molecular docking results showed that silanol-C18-ATMAC and C18-ATMAC exhibited similar binding affinities at Sudlow's site I (−6.04 and −6.09 kcal/mol, respectively), but silanol-C18-ATMAC demonstrated a significantly stronger interaction at Sudlow's site II (−6.62 and −7.01 kcal/mol, respectively) (Figure 3c), likely due to favorable interactions with LEU430 at this site (Figure S10).[78,79]

Although direct comparisons of half-life between silanol and carbon-based parent molecules are limited, accumulating evidence suggests enhanced bioaccumulation potential for silylated-modified compounds, which have been frequently applied in drug design. For instance, silperisone, which contains a quaternary ammonium group, has demonstrated prolonged duration and increased oral bioavailability.[77] These findings support that a silanol group in ATMAC structures can increase lipophilicity, potentially leading to prolonged plasma half-lives.

Concentrations of Silanol-ATMACs and Traditional QACs in Disinfectants and Indoor Dust

To better understand the distribution of silanol-ATMACs relative to traditional QACs across commercial disinfectants, we analyzed a series of popular products in the market (Figure S11). Initial comparisons across product forms (e.g., sprays, wipes, and liquids) and brands showed no consistent differences in the concentrations of silanol-ATMACs versus traditional QACs. However, a specific medical-grade (product 12) contained silanol-ATMACs at concentrations up to 5080 mg/L, while traditional QACs were present at relatively low concentrations (Figure S11). This observation motivates us to reclassify the products based on their intended uses, categorizing them into medical and household purposes.

All silanol-ATMACs were found in all of the collected medical disinfectants. The total concentration of silanol-ATMACs (∑silanol-ATMAC) ranged from 158 to 5080 mg/L in these products, with a median concentration of 779 mg/L, which was 4.4−52 times higher than corresponding levels of traditional BACs, DADMACs, and ATMACs (Table 1). In contrast, only two silanol-ATMACs, namely silanol-C16-ATMAC and silanol-C18-ATMAC, were detected in household disinfectants with detection frequencies of 20 and 100%, respectively. Compared to the levels of ∑silanol-ATMAC in the medical disinfectants, ∑silanol-ATMAC concentration declined to 4.58 mg/L in the household disinfectants, approximately 1−2 orders of magnitude lower than those of traditional QACs, such as BACs, DADMACs, and ATMACs (medians: 1180, 169, and 47.4 mg/L, respectively). Obviously, ∑silanol-ATMAC concentrations were significantly higher in medical disinfectants than in household disinfectants, indicating a predominant presence of silanol-ATMACs in medical-grade products ($p < 0.001$; Figure 4). No silane-ATMAC was detected in any of the disinfecting

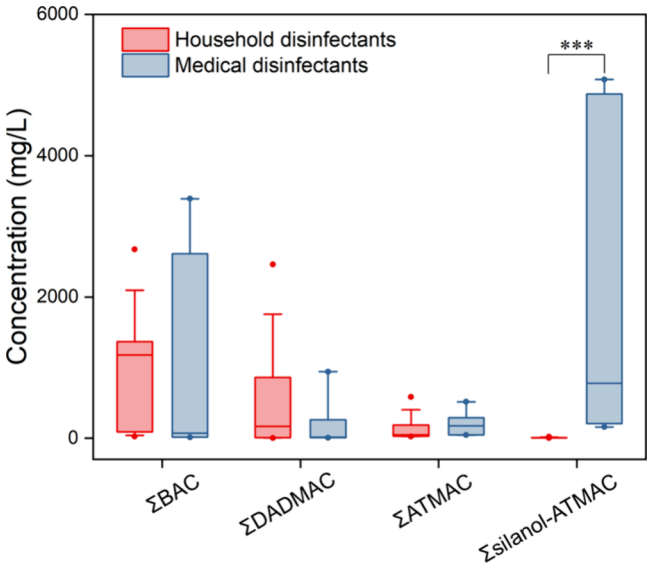

Figure 4. Concentrations of different groups of QACs in household and medical disinfectants (mg/L). Concentrations are shown as box plots, representing the 25th and 75th percentiles; black lines represent the median; the whiskers represent the 10th and 90th percentiles; and the dots represent the 5th and 95th percentiles. *** represents the statistical significance at $p < 0.001$.

products. To the best of our knowledge, silane-ATMACs were originally used as active commercial formulas in disinfectants to meet excellent antimicrobial functions. Due to their high reactive properties, these silane-ATMACs would hydrolyze into silanol-ATMACs in the presence of water. These results indicate that silanol-ATMACs are a transformation product of silane-ATMAC, rather than primary additives.

The composition profiles of traditional QACs, including BACs, DADMACs, and ATMACs in the household disinfectants were different from those reported in the products sold in the United States (84.2, 12.1, and 3.40% vs 64, 14, and 22%,

https://doi.org/10.1021/acs.est.5c13764
Environ. Sci. Technol. XXXX, XXX, XXX−XXX

respectively). These differences likely reflect variations in environmental conditions, usage patterns of cleaning and disinfecting products, and regulatory frameworks.[10] In total, traditional QACs dominated household disinfectants, accounting for 99.7% of the ∑QAC concentration, while a significant decline in the proportion of traditional QACs was observed in medical disinfectants, where silanol-ATMACs contributed up to 79.1% of the total QAC concentration (Figure 5). The different

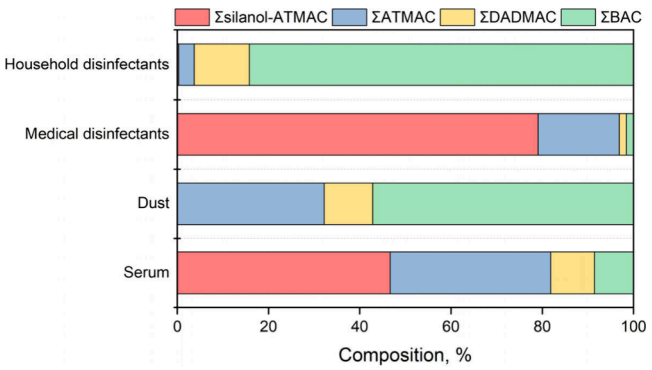

Figure 5. Comparison of contributions of four QAC groups to the ∑QAC concentrations in household disinfectants, medical disinfectants, residential dust, and human serum. Stacked bars show mean proportional composition.

profiles of traditional QACs and silanol-ATMACs in these disinfectants may be due to differences in their distinct functions, stemming from the active ingredients present in the analyzed products. This disparity aligns with literature indicating that household disinfectants favor shorter chain traditional QACs (e.g., C8−C16 BACs) for rapid action and low residue,[10] while medical formulations often incorporate organosilane QACs for their superior durability, covalent bonding to surfaces, and extended antimicrobial efficacy in high-risk environments like hospitals.[80,81] Such profiles may also reflect regulatory preferences, with medical disinfectants prioritizing nonvolatile, low-leaching compounds to minimize recontamination in sterile settings.[81] The detection of silanol-ATMACs in household disinfectants, albeit at relatively low concentrations, may result from their unintentional introduction as impurities associated with traditional QACs or from their intentional use as proprietary additives to enhance disinfecting performance.

Similarly, silanol-ATMACs were detected in all the dust samples, indicating that these newly identified chemicals are ubiquitously distributed in indoor environments. The ∑silanol-ATMAC concentrations ranged from 0.001 to 0.0886 μg/g with a median concentration of 0.00804 μg/g. The levels of ∑silanol-ATMACs were significantly lower than those of ∑traditional QACs (median: 35.9 μg/g; Table 1). To explore the potential source of silanol-ATMACs in residential dust, we compared the contributions of traditional QACs and silanol-ATMACs in the dust and products (Figure 5). Given that disinfectants were classified by their distinct application scenarios, only traditional QAC disinfectants were regularly used in the homes. Intriguingly, a similar pattern was observed in residential dust and household disinfectants (99.9 and 0.10% vs 99.7 and 0.30%), suggesting that these household disinfectants may have been heavily used in these homes. The lower but ubiquitous silanol-ATMAC residues in dust likely originate from household products, where they serve as minor additives that potentially migrate through aerosol deposition or wear from treated textiles and surfaces.

Concentrations of Silanol-ATMACs and Traditional QACs in Human Serum

To further validate the presence of these emerging QACs in human blood, a highly sensitive method was developed to analyze these chemicals using a pseudotargeted analysis strategy (see the chromatograms in Figure S12). As a result, silanol-C10-, C12-, C14-, C16-, and C18-ATMACs were detected in more than 88% of the samples with median concentrations of 1.18, 2.65, 0.102, 3.56, and 2.46 ng/mL, respectively. The ∑silanol-ATMAC concentrations ranged from 2.02 to 21.5 ng/mL with a median concentration of 10.6 ng/mL in the serum, generally higher than those of ∑BAC, ∑DADMAC, and ∑ATMAC (medians: 1.94, 2.16, and 7.96 ng/mL, respectively). Notably, significant differences in the profiles of traditional QACs and silanol-ATMACs were observed between the residential dust and human serum (99.9 and 0.10% vs 53.3 and 46.7%, respectively; Figure 5), suggesting that other factors and exposure pathways, rather than dust ingestion, may influence the body burden of these chemicals. This may be attributed to the use of silanol-ATMACs in wound disinfectants and textiles, leading to direct human exposure via dermal contact. In contrast to traditional QACs, which primarily enter the body through indirect pathways such as dietary intake or dust ingestion requiring translocation across the intestinal epithelium barrier,[82] silanol-ATMACs may exhibit higher absorption efficiency due to their direct dermal exposure route. Intriguingly, similar composition profiles of traditional QACs and silanol-ATMACs were found between the serum and the medical disinfectants (53.3 and 46.7% vs 20.9 and 79.1%, respectively; Figure 5). These results further suggest that medical disinfectants may serve as a significant source of silanol-ATMACs, resulting in widespread human exposure to these chemicals. This linkage is supported by evidence of organosilane QACs' use in medical settings for durable antimicrobial coatings on wounds, textiles, and surfaces,[68−70,75] where direct contact increases exposure risks, potentially contributing to health outcomes like skin irritation, asthma, or antimicrobial resistance in vulnerable populations.

■ ENVIRONMENTAL IMPLICATIONS

This study has several limitations. The sample size was small for both disinfectants and indoor dust samples. Besides, the dust and serum samples collected from limited geographic areas may not represent the general distribution characteristics of QACs in China. Thus, the findings in this study may require further validation and need to be exemplified with larger sample volumes to reveal the widespread existence of this compound in the indoor environment and human serum. Additionally, the levels of QACs and silanol-ATMACs may be overestimated through semi-quantification due to the lack of commercial standards.

Nonetheless, our present study has isolated bioaccumulative chemicals in disinfectants based on a PA-UF-MS strategy, which has successfully identified and prioritized thousands of HSA ligands. Given the structural diversity of QACs in production and use, the successful identification of silanol-ATMACs highlights the effectiveness of our PA-UF-MS strategy, particularly in analyzing complex environmental mixtures. In addition, a pseudo-MRM strategy was employed to quantify silanol-ATMACs in environmental matrices. This approach

https://doi.org/10.1021/acs.est.5c13764
Environ. Sci. Technol. XXXX, XXX, XXX−XXX

enables more reliable detection of these compounds and facilitates pathway-guided interpretation, thereby advancing our understanding of their environmental occurrence and potential health relevance. In this study, UF-MS was applied for the first time to screen potential novel bioaccumulative contaminants in real environmental samples. Although the technique has been widely used in fields such as pharmaceutical research for screening natural ligands, it has not previously been incorporated into the screening of unknown environmental contaminants. The two-filter strategy effectively reduces false negatives for amphiphilic compounds and shows strong capability for identifying bioaccumulative contaminants with mixed hydrophobic and hydrophilic characteristics. In addition, the increase in production and use of disinfectants would unavoidably lead to continuous contamination of QACs in the indoor environments. Furthermore, the identification of BACs as the high-affinity ligands of HSA is significant. This is due to comparing with other QAC groups, BACs were the predominant species among QAC groups detected in indoor dust and disinfectants.[3,4] Moreover, previous studies have demonstrated that BACs exert higher toxicity than other QAC groups.[83,84] Finally, it is worth noting that silanol-ATMAC homologues were identified in this study; further efforts are warranted to investigate their environmental occurrence, persistence, and potential toxicity.

■ ASSOCIATED CONTENT

Data Availability Statement

All raw mass spectrometry files are available as data set MSV000100350 at the GNPS MassIVE repository (https://massive.ucsd.edu/ProteoSAFe/static/massive.jsp), citable under DOI: 10.25345/C5959CN10 and accessible via ftp://massive-ftp.ucsd.edu/v11/MSV000100350.

Supporting Information

The Supporting Information is available free of charge at https://pubs.acs.org/doi/10.1021/acs.est.5c13764.

Details of instrumental analysis and quality control, hydrolysis and aqueous transformation of silane- and silanol-ATMACs, molecular docking and ITC analysis of QAC−HSA interactions, optimized MRMs, recoveries, matrix effects, and detection limits, protein affinity ultrafiltration−MS workflows and non-specific binding evaluation, identification and quantification of QACs and silanol-ATMACs in disinfectants, and additional chromatograms and supporting LC−MS/MS data (PDF)

■ AUTHOR INFORMATION

Corresponding Authors

Da Chen − *College of Environment and Climate, Guangdong Key Laboratory of Environmental Pollution and Health, Jinan University, Guangzhou 510632, China;* orcid.org/0000-0001-5563-0091; Email: dachen@jnu.edu.cn

Guomao Zheng − *State Key Laboratory of Soil Pollution Control and Safety, Shenzhen Key Laboratory of Precision Measurement and Early Warning Technology for Urban Environmental Health Risks, School of Environmental Science and Engineering, Southern University of Science and Technology, Shenzhen 518055, China;* orcid.org/0000-0002-5235-9950; Email: zhenggm@sustech.edu.cn

Authors

Yao Cheng − *State Key Laboratory of Soil Pollution Control and Safety, Shenzhen Key Laboratory of Precision Measurement and Early Warning Technology for Urban Environmental Health Risks, School of Environmental Science and Engineering, Southern University of Science and Technology, Shenzhen 518055, China; College of Environment and Climate, Guangdong Key Laboratory of Environmental Pollution and Health, Jinan University, Guangzhou 510632, China*

Zhong Lv − *State Key Laboratory of Soil Pollution Control and Safety, Shenzhen Key Laboratory of Precision Measurement and Early Warning Technology for Urban Environmental Health Risks, School of Environmental Science and Engineering, Southern University of Science and Technology, Shenzhen 518055, China*

Haoran Xia − *State Key Laboratory of Soil Pollution Control and Safety, Shenzhen Key Laboratory of Precision Measurement and Early Warning Technology for Urban Environmental Health Risks, School of Environmental Science and Engineering, Southern University of Science and Technology, Shenzhen 518055, China*

Xiaoyuan Guo − *State Key Laboratory of Soil Pollution Control and Safety, Shenzhen Key Laboratory of Precision Measurement and Early Warning Technology for Urban Environmental Health Risks, School of Environmental Science and Engineering, Southern University of Science and Technology, Shenzhen 518055, China*

Xiaozhen Zhang − *State Key Laboratory of Soil Pollution Control and Safety, Shenzhen Key Laboratory of Precision Measurement and Early Warning Technology for Urban Environmental Health Risks, School of Environmental Science and Engineering, Southern University of Science and Technology, Shenzhen 518055, China*

Baoqin Huang − *Department of Obstetrics, The Third Affiliated Hospital, Sun Yat-sen University, Guangzhou 510630, China*

Bixuan Wang − *School of Materials Science and Engineering, Beihang University, Beijing 100191, China*

Zhaomin Dong − *School of Materials Science and Engineering, Beihang University, Beijing 100191, China; School of Public Health, Southeast University, Nanjing 210009, China*

Complete contact information is available at: https://pubs.acs.org/10.1021/acs.est.5c13764

Author Contributions

†Yao Cheng and Zhong Lv contributed equally to this work.

Notes

The authors declare no competing financial interest.

■ ACKNOWLEDGMENTS

This study was financially supported by the National Natural Science Foundation of China (22206071, 22476080, and 42222710), the Shenzhen Science and Technology Program (KQTD20240729102048052 and 20231116225539001), and the High Level of Special Funds (G03034K006). The authors also thank Mengyao Ran and Dr. Haoqi Nina Zhao for their help with uploading the HRMS raw data.

■ REFERENCES

(1) Hora, P. I.; Pati, S. G.; McNamara, P. J.; Arnold, W. A. Increased Use of Quaternary Ammonium Compounds during the SARS-CoV-2

Pandemic and Beyond: Consideration of Environmental Implications. *Environ. Sci. Technol. Lett.* **2020**, *7*, 622−631.
(2) Marteinson, S. C.; Lawrence, M. J.; Taranu, Z. E.; Kosziwka, K.; Taylor, J. J.; Green, A.; Winegardner, A. K.; Rytwinski, T.; Reid, J. L.; Dubetz, C.; Leblanc, J.; Galus, M. D.; Cooke, S. J. Increased Use of Sanitizers and Disinfectants during the COVID-19 Pandemic: Identification of Antimicrobial Chemicals and Considerations for Aquatic Environmental Contamination. *Environ. Rev.* **2023**, *31*, 76−94.
(3) Zheng, G.; Filippelli, G. M.; Salamova, A. Increased Indoor Exposure to Commonly Used Disinfectants during the COVID-19 Pandemic. *Environ. Sci. Technol. Lett.* **2020**, *7*, 760−765.
(4) Cheng, Y.; Liu, C.; Lv, Z.; Liang, Y.; Xie, Y.; Wang, C.; Wan, S.; Leng, X.; Hu, M.; Zheng, G. High-Resolution Mass Spectrometry Screening of Quaternary Ammonium Compounds (QACs) in Dust from Homes and Various Microenvironments in South China. *Environ. Sci. Technol.* **2024**, *58*, 3182−3193.
(5) Belova, L.; Poma, G.; Roggeman, M.; Jeong, Y.; Kim, D.-H.; Berghmans, P.; Peters, J.; Salamova, A.; van Nuijs, A. L. N.; Covaci, A. Identification and Characterization of Quaternary Ammonium Compounds in Flemish Indoor Dust by Ion-Mobility High-Resolution Mass Spectrometry. *Environ. Int.* **2023**, *177*, No. 108021.
(6) Zheng, G.; Webster, T. F.; Salamova, A. Quaternary Ammonium Compounds: Bioaccumulation Potentials in Humans and Levels in Blood before and during the Covid-19 Pandemic. *Environ. Sci. Technol.* **2021**, *55*, 14689−14698.
(7) Li, Z.-M.; Kannan, K. Quaternary Ammonium Compounds in Paired Human Urine and Feces: Relative Significance of Biliary Elimination. *Environ. Sci. Technol. Lett.* **2024**, *11*, 533−538.
(8) Zheng, G.; Schreder, E.; Sathyanarayana, S.; Salamova, A. The First Detection of Quaternary Ammonium Compounds in Breast Milk: Implications for Early-Life Exposure. *J. Expo. Sci. Environ. Epidemiol.* **2022**, *32*, 682−688.
(9) Hu, M.; Li, L.; Lv, Z.; Sangion, A.; Zheng, G.; Cai, Z.; Salamova, A. Quaternary Ammonium Compounds in Paired Samples of Blood and Indoor Dust from the United States. *Environ. Sci. Technol. Lett.* **2024**, *11*, 1308−1313.
(10) Arnold, W. A.; Blum, A.; Branyan, J.; Bruton, T. A.; Carignan, C. C.; Cortopassi, G.; Datta, S.; DeWitt, J.; Doherty, A.-C.; Halden, R. U.; Harari, H.; Hartmann, E. M.; Hrubec, T. C.; Iyer, S.; Kwiatkowski, C. F.; LaPier, J.; Li, D.; Li, L.; Muñiz Ortiz, J. G.; Salamova, A.; Schettler, T.; Seguin, R. P.; Soehl, A.; Sutton, R.; Xu, L.; Zheng, G. Quaternary Ammonium Compounds: A Chemical Class of Emerging Concern. *Environ. Sci. Technol.* **2023**, *57*, 7645−7665.
(11) Meylan, W. M.; Howard, P. H.; Boethling, R. S.; Aronson, D.; Printup, H.; Gouchie, S. Improved Method for Estimating Bioconcentration/Bioaccumulation Factor from Octanol/Water Partition Coefficient. *Environ. Toxicol. Chem.* **1999**, *18*, 664−672.
(12) Organisation for Economic Co-operation and Development (OECD). OECD Guidelines for the Testing of Chemicals. *Magnit. Pestic. Residues Process. Commod.* **1997**, *508*, 15.
(13) Maciążek-Jurczyk, M.; Szkudlarek, A.; Chudzik, M.; Pożycka, J.; Sułkowska, A. Alteration of Human Serum Albumin Binding Properties Induced by Modifications: A Review. *Spectrochim. Acta. A. Mol. Biomol. Spectrosc.* **2018**, *188*, 675−683.
(14) Rabbani, G.; Ahn, S. N. Structure, Enzymatic Activities, Glycation and Therapeutic Potential of Human Serum Albumin: A Natural Cargo. *Int. J. Biol. Macromol.* **2019**, *123*, 979−990.
(15) Fan, J.; Gilmartin, K.; Octaviano, S.; Villar, F.; Remache, B.; Regan, J. Using Human Serum Albumin Binding Affinities as a Proactive Strategy to Affect the Pharmacodynamics and Pharmacokinetics of Preclinical Drug Candidates. *ACS Pharmacol. Transl. Sci.* **2022**, *5*, 803−810.
(16) Rehman, M. T.; Khan, A. U. Understanding the Interaction Between Human Serum Albumin and Anti-Bacterial/Anti-Cancer Compounds. *Curr. Pharm. Des.* **2015**, *21*, 1785−1799.
(17) Song, H.-P.; Zhang, H.; Fu, Y.; Mo, H.; Zhang, M.; Chen, J.; Li, P. Screening for Selective Inhibitors of Xanthine Oxidase from Flos Chrysanthemum Using Ultrafiltration LC−MS Combined with Enzyme Channel Blocking. *J. Chromatogr. B* **2014**, *961*, 56−61.
(18) Wang, L.; Chen, M.; Sun, Q.; Yang, Y.; Rong, R. Discovery of the Potential Neuraminidase Inhibitors from *Polygonum cuspidatum* by Ultrafiltration Combined with Mass Spectrometry Guided by Molecular Docking. *J. Sep. Sci.* **2023**, *46*, No. 2200937.
(19) Zhang, H.; Xu, C.; Tian, Q.; Zhang, Y.; Zhang, G.; Guan, Y.; Tong, S.; Yan, J. Screening and Characterization of Aldose Reductase Inhibitors from Traditional Chinese Medicine Based on Ultrafiltration-Liquid Chromatography Mass Spectrometry and in Silico Molecular Docking. *J. Ethnopharmacol.* **2021**, *264*, No. 113282.
(20) Li, Y.-J.; Wan, G.-Z.; Xu, F.-C.; Guo, Z.-H.; Chen, J. Screening and Identification of α-Glucosidase Inhibitors from Cyclocarya Paliurus Leaves by Ultrafiltration Coupled with Liquid Chromatography-Mass Spectrometry and Molecular Docking. *J. Chromatogr. A* **2022**, *1675*, No. 463160.
(21) Yang, M.; Ni, L.; Wang, Y.; Xuan, Z.; Wu, H.; Zhan, W.; Wan, X.; Wang, J.; Xu, F. Screening Bioactive Compounds from Danggui-Shaoyao-San for Treating Sodium Retention in Nephrotic Syndrome Using Bio-Affinity Ultrafiltration. *J. Ethnopharmacol.* **2022**, *292*, No. 115171.
(22) Wang, H.-P.; Fan, C.-L.; Lin, Z.-Z.; Yin, Q.; Zhao, C.; Peng, P.; Zhang, R.; Wang, Z.-J.; Du, J.; Wang, Z.-B. Screening of Potential α-Glucosidase Inhibitors from the Roots and Rhizomes of Panax Ginseng by Affinity Ultrafiltration Screening Coupled with UPLC-ESI-Orbitrap-MS Method. *Molecules* **2023**, *28*, 2069.
(23) Wang, S.; Huai, J.; Shang, Y.; Xie, L.; Cao, X.; Liao, J.; Zhang, T.; Dai, R. Screening for Natural Inhibitors of 5-Lipoxygenase from Zi-Shen Pill Extract by Affinity Ultrafiltration Coupled with Ultra Performance Liquid Chromatography-Mass Spectrometry. *J. Ethnopharmacol.* **2020**, *254*, No. 112733.
(24) Wang, X.; Liu, Q.; Zhong, W.; Yang, L.; Yang, J.; Covaci, A.; Zhu, L. Estimating Renal and Hepatic Clearance Rates of Organophosphate Esters in Humans: Impacts of Intrinsic Metabolism and Binding Affinity with Plasma Proteins. *Environ. Int.* **2020**, *134*, No. 105321.
(25) Beesoon, S.; Martin, J. W. Isomer-Specific Binding Affinity of Perfluorooctanesulfonate (PFOS) and Perfluorooctanoate (PFOA) to Serum Proteins. *Environ. Sci. Technol.* **2015**, *49*, 5722−5731.
(26) Zhang, H.; Xu, C.; Tian, Q.; Zhang, Y.; Zhang, G.; Guan, Y.; Tong, S.; Yan, J. Screening and Characterization of Aldose Reductase Inhibitors from Traditional Chinese Medicine Based on Ultrafiltration-Liquid Chromatography Mass Spectrometry and *in Silico* Molecular Docking. *J. Ethnopharmacol.* **2021**, *264*, No. 113282.
(27) Cieśla, Ł.; Moaddel, R. Comparison of Analytical Techniques for the Identification of Bioactive Compounds from Natural Products. *Nat. Prod. Rep.* **2016**, *33*, 1131−1145.
(28) Curry, S.; Brick, P.; Franks, N. P. Fatty Acid Binding to Human Serum Albumin: New Insights from Crystallographic Studies. *Biochim. Biophys. Acta BBA - Mol. Cell Biol. Lipids* **1999**, *1441*, 131−140.
(29) Sheng, N.; Li, J.; Liu, H.; Zhang, A.; Dai, J. Interaction of Perfluoroalkyl Acids with Human Liver Fatty Acid-Binding Protein. *Arch. Toxicol.* **2016**, *90*, 217−227.
(30) Karvellas, C. J.; Speiser, J. L.; Tremblay, M.; Lee, W. M.; Rose, C. F. Elevated FABP1 Serum Levels Are Associated with Poorer Survival in Acetaminophen-induced Acute Liver Failure. *Hepatology* **2017**, *65*, 938−949.
(31) Ren, X.-M.; Qin, W.-P.; Cao, L.-Y.; Zhang, J.; Yang, Y.; Wan, B.; Guo, L.-H. Binding Interactions of Perfluoroalkyl Substances with Thyroid Hormone Transport Proteins and Potential Toxicological Implications. *Toxicology* **2016**, *366*−*367*, 32−42.
(32) Fanali, G.; di Masi, A.; Trezza, V.; Marino, M.; Fasano, M.; Ascenzi, P. Human Serum Albumin: From Bench to Bedside. *Mol. Aspects Med.* **2012**, *33*, 209−290.
(33) Zhang, L.; Yang, P.; Shu, Y.; Huang, W.; Sun, W.; Liu, X.; Chen, D. Suspect-Screening Analysis of Environmental Chemicals in Paired Human Cerebrospinal Fluid and Serum Samples. *Environ. Health Perspect.* **2024**, *132*, No. 047701.
(34) Tang, S.; Sun, X.; Qiao, X.; Cui, W.; Yu, F.; Zeng, X.; Covaci, A.; Chen, D. Prenatal Exposure to Emerging Plasticizers and Synthetic Antioxidants and Their Potency to Cross Human Placenta. *Environ. Sci. Technol.* **2022**, *56*, 8507−8517.

https://doi.org/10.1021/acs.est.5c13764
Environ. Sci. Technol. XXXX, XXX, XXX−XXX

(35) Liu, D.; Guo, J.; Luo, Y.; Broderick, D. J.; Schimerlik, M. I.; Pezzuto, J. M.; van Breemen, R. B. Screening for Ligands of Human Retinoid X Receptor-α Using Ultrafiltration Mass Spectrometry. *Anal. Chem.* **2007**, *79*, 9398−9402.
(36) Banker, M. J.; Clark, T. H. Plasma/Serum Protein Binding Determinations. *Curr. Drug Metab.* **2008**, *9*, 854−859.
(37) Kurkov, S. V.; Loftsson, T.; Messner, M.; Madden, D. Parenteral Delivery of HPβCD: Effects on Drug-HSA Binding. *AAPS PharmSciTech* **2010**, *11*, 1152−1158.
(38) Schymanski, E. L.; Singer, H. P.; Longrée, P.; Loos, M.; Ruff, M.; Stravs, M. A.; Ripollés Vidal, C.; Hollender, J. Strategies to Characterize Polar Organic Contamination in Wastewater: Exploring the Capability of High Resolution Mass Spectrometry. *Environ. Sci. Technol.* **2014**, *48*, 1811−1818.
(39) Zheng, J.; Yang, J.; Zhao, F.; Peng, B.; Wang, Y.; Fang, M. CIL-ExPMRM: An Ultrasensitive Chemical Isotope Labeling Assisted Pseudo-MRM Platform to Accelerate Exposomic Suspect Screening. *Environ. Sci. Technol.* **2023**, *57*, 10962−10973.
(40) Hayhow, T. G.; Williamson, B.; Lawson, M.; Cureton, N.; Braybrooke, E. L.; Campbell, A.; Carbajo, R. J.; Cheraghchi-Bashi, A.; Chiarparin, E.; Diène, C. R.; Fallan, C.; Fisher, D. I.; Goldberg, F. W.; Hopcroft, L.; Hopcroft, P.; Jackson, A.; Kettle, J. G.; Klinowska, T.; Künzel, U.; Lamont, G.; Lewis, H. J.; Maglennon, G.; Martin, S.; Gutierrez, P. M.; Morrow, C. J.; Nikolaou, M.; Nissink, J. W. M.; O'Shea, P.; Polanski, R.; Schade, M.; Scott, J. S.; Smith, A.; Weber, J.; Wilson, J.; Yang, B.; Crafter, C. Metabolism-Driven in Vitro/in Vivo Disconnect of an Oral ERα VHL-PROTAC. *Commun. Biol.* **2024**, *7*, 563.
(41) Zhao, L.; Thongrakon, B.; Gautom, T.; Sahlberg, V.; Berglund, P. Exploring the Stability and Substrate Profile of Transaminase from *Silicibacter pomeroyi* with Ancestral Sequence Reconstruction. *ChemBioChem* **2025**, *26*, No. 2500155.
(42) Eberhardt, J.; Santos-Martins, D.; Tillack, A. F.; Forli, S. AutoDock Vina 1.2.0: New Docking Methods, Expanded Force Field, and Python Bindings. *J. Chem. Inf. Model.* **2021**, *61*, 3891−3898.
(43) Ng, C. A.; Hungerbühler, K. Exploring the Use of Molecular Docking to Identify Bioaccumulative Perfluorinated Alkyl Acids (PFAAs). *Environ. Sci. Technol.* **2015**, *49*, 12306−12314.
(44) Lee, P.; Wu, X. Modifications of Human Serum Albumin and Their Binding Effect. *Curr. Pharm. Des.* **2015**, *21*, 1862−1865.
(45) Srivastava, R.; Alam, Md. S. Spectroscopic Studies of the Aggregation Behavior of Human Serum Albumin and Cetyltrimethylammonium Bromide. *Int. J. Biol. Macromol.* **2020**, *158*, 394−400.
(46) Wang, Q.; Chang, K.-L.; Fan, J.-W.; Xu, S.-H.; Yan, C.-G. Construction of a Human Serum Albumin Site II-Targeting Supramolecular Fluorescent Probe for Cell Imaging and Drug Delivery. *J. Mol. Struct.* **2024**, *1312*, No. 138503.
(47) Peltenburg, H.; Bosman, I. J.; Hermens, J. L. M. Sensitive Determination of Plasma Protein Binding of Cationic Drugs Using Mixed-Mode Solid-Phase Microextraction. *J. Pharm. Biomed. Anal.* **2015**, *115*, 534−542.
(48) Liu, D.; Guo, J.; Luo, Y.; Broderick, D. J.; Schimerlik, M. I.; Pezzuto, J. M.; van Breemen, R. B. Screening for Ligands of Human Retinoid X Receptor-α Using Ultrafiltration Mass Spectrometry. *Anal. Chem.* **2007**, *79*, 9398−9402.
(49) Curry, S.; Mandelkow, H.; Brick, P.; Franks, N. Crystal Structure of Human Serum Albumin Complexed with Fatty Acid Reveals an Asymmetric Distribution of Binding Sites. *Nat. Struct. Biol.* **1998**, *5*, 827−835.
(50) Ullah, A.; Shin, G.; Lim, S. I. Human Serum Albumin Binders: A Piggyback Ride for Long-Acting Therapeutics. *Drug Discovery Today* **2023**, *28*, No. 103738.
(51) Zenei, T.; Hiroshi, T. Specific and Non-Specific Ligand Binding to Serum Albumin. *Biochem. Pharmacol.* **1985**, *34*, 1999−2005.
(52) Kowalska, D.; Stolte, S.; Wyrzykowski, D.; Stepnowski, P.; Dołżonek, J. Interaction of Ionic Liquids with Human Serum Albumin in the View of Bioconcentration: A Preliminary Study. *Chem. Pap.* **2022**, *76*, 2405−2417.
(53) Crisalli, A. M.; Cai, A.; Cho, B. P. Probing the Interactions of Perfluorocarboxylic Acids of Various Chain Lengths with Human Serum Albumin: Calorimetric and Spectroscopic Investigations. *Chem. Res. Toxicol.* **2023**, *36*, 703−713.
(54) Bratty, M. A. Spectroscopic and Molecular Docking Studies for Characterizing Binding Mechanism and Conformational Changes of Human Serum Albumin upon Interaction with Telmisartan. *Saudi Pharm. J. SPJ. Off. Publ. Saudi Pharm. Soc.* **2020**, *28*, 729−736.
(55) Zhao, L.; Teng, M.; Zhao, X.; Li, Y.; Sun, J.; Zhao, W.; Ruan, Y.; Leung, K. M. Y.; Wu, F. Insight into the Binding Model of Per- and Polyfluoroalkyl Substances to Proteins and Membranes. *Environ. Int.* **2023**, *175*, No. 107951.
(56) Crisalli, A. M.; Cai, A.; Cho, B. P. Probing the Interactions of Perfluorocarboxylic Acids of Various Chain Lengths with Human Serum Albumin: Calorimetric and Spectroscopic Investigations. *Chem. Res. Toxicol.* **2023**, *36*, 703−713.
(57) Bissantz, C.; Kuhn, B.; Stahl, M. A Medicinal Chemist's Guide to Molecular Interactions. *J. Med. Chem.* **2010**, *53*, 5061−5084.
(58) Sivertsen, A.; Isaksson, J.; Leiros, H.-K. S.; Svenson, J.; Svendsen, J.-S.; Brandsdal, B. O. Synthetic Cationic Antimicrobial Peptides Bind with Their Hydrophobic Parts to Drug Site II of Human Serum Albumin. *BMC Struct. Biol.* **2014**, *14*, 4.
(59) Costa-Tuna, A.; Chaves, O. A.; Almeida, Z. L.; Cunha, R. S.; Pina, J.; Serpa, C. Profiling the Interaction between Human Serum Albumin and Clinically Relevant HIV Reverse Transcriptase Inhibitors. *Viruses* **2024**, *16*, 491.
(60) Zhuo, W.; Peng, X.; Lin, X. Insights into the Interaction Mechanism between Tiagabine Hydrochloride and Two Serum Albumins. *RSC Adv.* **2018**, *8*, 24953−24960.
(61) Vuignier, K.; Schappler, J.; Veuthey, J.-L.; Carrupt, P.-A.; Martel, S. Drug−Protein Binding: A Critical Review of Analytical Tools. *Anal. Bioanal. Chem.* **2010**, *398*, 53−66.
(62) Kumar, S.; Mitra, R.; Ayyannan, S. R. Design, Synthesis and Evaluation of Benzothiazole-Derived Phenyl Thioacetamides as Dual Inhibitors of Monoamine Oxidases and Cholinesterases. *Mol. Divers.* **2025**, *29*, 4231−4253.
(63) Yang, Y.; Liu, J.; Wang, Y.; Wu, X.; Li, L.; Bian, G.; Li, W.; Yuan, H.; Zhang, Q. Blockade of Pre-Synaptic and Post-Synaptic GABAB Receptors in the Lateral Habenula Produces Different Effects on Anxiety-like Behaviors in 6-Hydroxydopamine Hemiparkinsonian Rats. *Neuropharmacology* **2021**, *196*, No. 108705.
(64) Torkelson, A. A.; da Silva, A. K.; Love, D. C.; Kim, J. Y.; Alper, J. P.; Coox, B.; Dahm, J.; Kozodoy, P.; Maboudian, R.; Nelson, K. L. Investigation of Quaternary Ammonium Silane-Coated Sand Filter for the Removal of Bacteria and Viruses from Drinking Water. *J. Appl. Microbiol.* **2012**, *113*, 1196−1207.
(65) Krieble, R. H.; Elliott, J. R. The Hydrolytic Cleavage of Methyl and Chloromethyl Siloxanes. *J. Am. Chem. Soc.* **1946**, *68*, 2291−2294.
(66) Osterholtz, F. D.; Pohl, E. R. Kinetics of the Hydrolysis and Condensation of Organofunctional Alkoxysilanes: A Review. *J. Adhes. Sci. Technol.* **1992**, *6*, 127−149.
(67) Speier, J. Development of an Organosilicone Antimicrobial Agent for the Treatment of Surfaces. *J. Coat. Fabr.* **1982**, *12*, 38−45.
(68) Ludwig, J. H.; Ohlhausen, H. Solvent-Free Organosilane Quaternary Ammonium Compositions, Method of Making and Use. U.S. Patent 8,735,618 B2, May 27, 2014.
(69) Eddy, C. A.; Eddy, P. Sanitizing and Antimicrobial Solution with Silane Quaternary Ammonium with Hypochlorous Acid. AU Patent 2020267176 A1, May 27, 2021.
(70) Eddy, P. E. Antimicrobial Treatment for a Healthcare Facility Headwall. U.S. Patent 20200095775 A1, March 26, 2020.
(71) Messaoud, M.; Chadeau, E.; Chaudouët, P.; Oulahal, N.; Langlet, M. Quaternary Ammonium-Based Composite Particles for Antibacterial Finishing of Cotton-Based Textiles. *J. Mater. Sci. Technol.* **2014**, *30*, 19−29.
(72) Lü, T.; Zhang, X.; Ma, R.; Qi, D.; Sun, Y.; Zhang, D.; Huang, J.; Zhao, H. Quaternary Ammonium Siloxane-Decorated Magnetic Nanoparticles for Emulsified Oil-Water Separation. *Sep. Purif. Technol.* **2023**, *309*, No. 123097.

https://doi.org/10.1021/acs.est.5c13764
Environ. Sci. Technol. XXXX, XXX, XXX−XXX

(73) Liu, X.-L.; Chen, Y.-F.; Chen, Y.-W.; Peng, W.-K.; Liu, H.-C. Preparation of Carbosilane Quaternary Ammonium Surfactants and Surface Activity. *Tenside Surfactants Deterg.* **2022**, *59*, 424−432.
(74) Shang, H.; Liu, J.; Zheng, Y.; Wang, L. Synthesis, Characterization, and Flocculation Properties of Poly(Acrylamide-Methacryloxyethyltrimethyl Ammonium Chloride-Methacryloxypropyltrimethoxy Silane). *J. Appl. Polym. Sci.* **2009**, *111*, 1594−1599.
(75) *KBM-9418−40|Shin-Etsu Silicone Selection Guide*; https://www.shinetsusilicone-global.com/guide/silanecoup/kbm-9418-40/ (accessed Dec 30, 2025).
(76) Wang, B.; Li, Y.; Zheng, J.; Fan, W.; Wang, Y.; Ma, F.; Chen, M.; Dong, Z. Using Stacking Ensemble Machine Learning to Estimate the Human Half-Life and Apparent Volume of Distribution: Implications for Human Health Risk Assessment. *ACS Chem. Health Saf.* **2025**, *32*, 810−825.
(77) Panayides, J.-L.; Riley, D. L.; Hasenmaile, F.; Van Otterlo, W. A. The Role of Silicon in Drug Discovery: A Review. *RSC Med. Chem.* **2024**, *15*, 3286−3344.
(78) Qiu, L.; Lin, J.; Liu, Q.; Wang, S.; Lv, G.; Li, K.; Shi, H.; Huang, Z.; Bertaccini, E. J. The Role of the Hydroxyl Group in Propofol−Protein Target Recognition: Insights from ONIOM Studies. *J. Phys. Chem. B* **2017**, *121*, 5883−5896.
(79) Daneshamouz, S.; Saadati, S.; Abdelrasoul, A. Molecular Docking Study of Biocompatible Enzyme Interactions for Removal of Indoxyl Sulfate (IS), Indole-3-Acetic Acid (IAA), and p-Cresyl Sulfate (PCS) Protein Bound Uremic Toxins. *Struct. Chem.* **2022**, *33*, 1133−1148.
(80) Bapat, R. A.; Parolia, A.; Chaubal, T.; Yang, H. J.; Kesharwani, P.; Phaik, K. S.; Lin, S. L.; Daood, U. Recent Update on Applications of Quaternary Ammonium Silane as an Antibacterial Biomaterial: A Novel Drug Delivery Approach in Dentistry. *Front. Microbiol.* **2022**, *13*, No. 927282.
(81) Boyce, J. M. Quaternary Ammonium Disinfectants and Antiseptics: Tolerance, Resistance and Potential Impact on Antibiotic Resistance. *Antimicrob. Resist. Infect. Control* **2023**, *12*, 32.
(82) Luz, A.; DeLeo, P.; Pechacek, N.; Freemantle, M. Human Health Hazard Assessment of Quaternary Ammonium Compounds: Didecyl Dimethyl Ammonium Chloride and Alkyl (C12−C16) Dimethyl Benzyl Ammonium Chloride. *Regul. Toxicol. Pharmacol.* **2020**, *116*, No. 104717.
(83) Braun, G.; Herberth, G.; Krauss, M.; König, M.; Wojtysiak, N.; Zenclussen, A. C.; Escher, B. I. Neurotoxic Mixture Effects of Chemicals Extracted from Blood of Pregnant Women. *Science* **2024**, *386*, 301−309.
(84) Cohn, E. F.; Clayton, B. L. L.; Madhavan, M.; Lee, K. A.; Yacoub, S.; Fedorov, Y.; Scavuzzo, M. A.; Paul Friedman, K.; Shafer, T. J.; Tesar, P. J. Pervasive Environmental Chemicals Impair Oligodendrocyte Development. *Nat. Neurosci.* **2024**, *27*, 836−845.

https://doi.org/10.1021/acs.est.5c13764
Environ. Sci. Technol. XXXX, XXX, XXX−XXX